Available online at www.sciencedirect.com
SCIENCE DIRECT
Polymer 46 (2005) 8774–8789
polymer
www.elsevier.com/locate/polymer

# Linear growth rates of random propylene ethylene copolymers. The changeover from γ dominated growth to mixed (α+γ) polymorphic growth

Rufina G. Alamo*, Anindya Ghosal, Jhunu Chatterjee, Kimberly L. Thompson

*Department of Chemical and Biomedical Engineering, Florida Agricultural and Mechanical University and Florida State University, 2525 Pottsdamer Street, Tallahassee, FL 32310-6046, USA*

Received 15 November 2004; received in revised form 10 February 2005; accepted 17 February 2005
Available online 5 July 2005

**Abstract**

The spherulitic linear growth rates of a homo-poly(propylene) and a series of propylene–ethylene copolymers, all synthesized with the same type of metallocene catalyst were analyzed. The inter-chain distribution of comonomer content is uniform in these copolymers and the intra-chain distribution adheres to the random behavior. Furthermore, the concentration of stereo and regio defects is constant for all copolymers. Thus, with these polymers it was possible to investigate the influence of ethylene content on the crystallization kinetics, as extracted from their linear growth rates. All iPPs investigated display mixed polymorphic behavior during isothermal crystallization and major emphasis was given to integrate the simultaneous development of the α and γ polymorphs, and their intimate structural relations during growth, in the analysis of the crystallization kinetics. A sharp break in spherulitic growth is found between times domains of mixed α+γ growth and growth of pure γ crystals reflecting a drastic change in growth mechanisms at the point where α development ceases. The rates corresponding to α growth are significantly higher than those characteristics of γ growth. In addition, growth data in the domain of mixed α+γ growth, which, following the structural models for α and γ branching, reflect the growth pattern of α crystals, display a discontinuity in the temperature gradient at the changeover from growth of mixed α+γ to γ dominated growth. This behavior correlates with that found in other systems that undergo a similar extended chain to folded change in crystallization mechanisms. The temperature coefficient of the linear growth rates is analyzed according to regime theory for both domains of growth. The results allow a quantitative framework for discussion of the interfacial free energies of α and γ crystals obtained from this analysis.


*Keywords:* Poly(propylene) copolymers; Crystallization kinetics; Poly(propylene) polymorphs

## 1. Introduction

Small contents of 1-alkene type comonomers are added via random copolymerization to the isotactic polypropylene chain to increase impact strength, ductility and transparency of these materials for applications where the reduction of crystallinity, melting point and stiffness, compared to the homopolymers values are not of concern. The co-units are structural irregularities that affect the crystallization behavior of poly(propylenes).

Studies of the crystallization kinetics of propylene ethylene copolymers have been carried out in earlier works using either unfractionated polydispersed samples [1,2] or fractions obtained from copolymers synthesized with similar types of Ziegler–Natta (ZN) catalysts [3,4]. It is well known that ZN catalysts lead to copolymers with a broad inter-chain distribution of the comonomer [4–6] while the intra-chain distribution may deviate from the random behavior [7]. The highest molecular weight species contain the least number of defects and vice versa [4–6]. Therefore, studies using unfractionated ZN-type copolymers are hampered by overlapping and opposed effects of comonomer content and molecular mass on crystallization rates. The broad inter-chain compositional heterogeneity is greatly reduced by fractionation. However, disparity in molar mass between the fractions remains, making it

* Corresponding author.
*E-mail address:* alamo@eng.fsu.edu (R.G. Alamo).

0032-3861/$ - see front matter © 2005 Elsevier Ltd. All rights reserved.
doi:10.1016/j.polymer.2005.02.128

difficult to study the contribution of the comonomer independently from that given by other variables of chain structure. It is not surprising that widely different behaviors, with respect to the contribution of the comonomer, have been reported in the literature. For example, the crystallization rates of ZN fractions studied by Gedde et al. [3] were not proportional to the concentration of comonomer while the copolymer fractions studied by Feng et al. [4] and by Avella et al. [2] displayed the expected decrease in the rate with increase of ethylene, as a structural irregularity in the chain. Tied relationships between comonomer composition and molecular weight of copolymers of the ZN type are difficult to overcome, even after fractionation, and are the cause of the non uniformity in the observed behavior.

Remarkable advances in understanding and controlling the chemical geometry of well defined coordination compounds in polymerization catalysis has led to new polyolefins which are inaccessible through conventional heterogeneous ZN catalysts [8–11]. In relation to the present work, random propylene copolymers can now be synthesized with metallocene catalysts that yield more uniformly distributed materials [12]. In these copolymers the molecular mass distribution is close to a most probable one, the inter-chain distribution of the comonomer content is narrow and, intra-molecularly, the comonomer is randomly distributed [13]. In addition, the content of the comonomer incorporated can be changed in a wide range while molecular mass and the concentration of stereo and regio irregularities is maintained constant in the new copolymers.

The influence of the ethylene content on the crystallization kinetics of random propylene ethylene copolymers can now be evaluated independently from the effects inferred by molecular weight or the presence of different concentrations of stereo or regio defects. In this paper we study the linear growth rates of a series of these novel propylene ethylene copolymers with a content of ethylene ranging from 0.8 to 7.5 mol%. Comparative analysis with kinetic data on ZN fractions of matched ethylene concentration will substantiate the strong effect of the defect distribution on the crystallization behavior [7]. Our previous extensive studies carried out in the same series of copolymers provide key polymorphic and morphological background for the analysis of the linear growth rates using nucleation theory [13,14]. In addition, the partitioning of the ethylene units between the crystalline and non-crystalline regions was obtained by solid state $^{13}C$ NMR [15] using a procedure that involves cross polarization under MAS. The results allow a better estimation of the equilibrium melting temperature of each copolymer, a critical parameter in the kinetic analysis.

A characteristic of the isothermal crystallization of random propylene copolymers is the development of a mixed ($\alpha+\gamma$) polymorphic behavior [13]. Both polymorphs are formed at the initial stages of the crystallization, however, the relative content of each phase changes continuously during crystallization [13]. After complete transformation, higher contents of the $\alpha$ (monoclinic) phase are developed in copolymers with low concentration of structural irregularities and in the low crystallization temperature region [13,16]. The lamellar morphology associated with the $\alpha$ form is unusual in that nearly normal $\alpha$ branching develops via homoepitaxial growth from a 'parent' lamellae. Profuse $\alpha$ branching leads to a characteristic cross-hatched lamellar morphology [17–20].

Increasing concentration of comonomer or any other structural irregularities and/or increasing crystallization temperature favors the formation of the $\gamma$ (orthothombic) phase [13,16]. The crystal structure of this phase is unprecedented for crystalline polymers in that the molecular chains do not follow the classical parallel arrangements in the lattice. The $\gamma$ phase comprises non-parallel chains tilted at 40° to the lamellae normal [21]. An important structural relation between both polymorphs was provided by evidencing the efficiency of the (0 1 0) $\alpha$ planes as surfaces for epitaxial $\gamma$ branching [22–24]. The schematics of lamellar growth with simultaneous $\alpha+\gamma$ branching, according to the suggested structural models [17,22], were given in our previous paper [14]. They are reproduced again in Fig. 1 to facilitate the discussion of the growth kinetics. Following this model, $\gamma$ lamellae have been observed to branch from $\alpha$ surfaces at a very high tilt angle (40°) [22]. When gamma crystallinity prevails, alpha lamellae oriented in the direction of the spherulitic radius are replaced by parallel arrays of short lamellae that appear transverse to the spherulitic radius. These arrays of short lamellae are the dominant features in the AFM images of iPPs with contents of $\gamma$ phase $> \sim 50\%$ following expectations based on the model of Fig. 1 [14]. The preferred growth directions for both phases have also been established and will be of relevance in the analysis of the spherulitic linear growth rates in conditions where both polymorphs are operative. Growth proceeds via the $a^*$ axis, perpendicular to the (1 1 0) plane of the $\alpha$ phase [25] and proceeds via the $c$ axis in the gamma [17,22]. With parent $\alpha$ lamellae oriented in the spherulitic radial direction, $\gamma$ branching outgrows at a 40° tilt from the (0 1 0) $\alpha$ phase. As a consequence, during simultaneous $\alpha+\gamma$ growth, the measurements of spherulitic radius with crystallization time should reflect the growth of $\alpha$ lamellae.

In the present work, the analysis of the kinetics of the linear growth rates is carried out integrating the simultaneous development of both polymorphs and their structural relations during isothermal growth.

## 2. Experimental section

### 2.1. Materials

Four experimental propylene ethylene copolymers obtained with the same bridged metallocene catalyst [13]

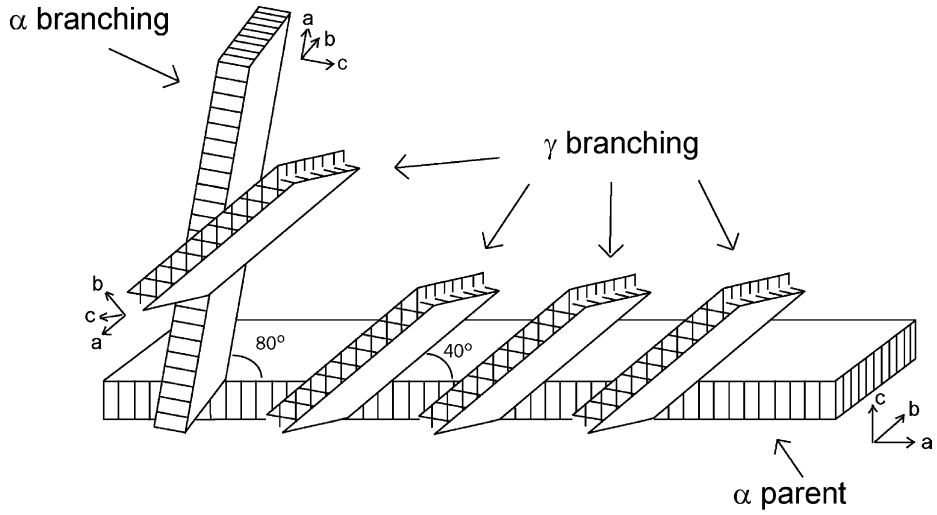


Fig. 1. Schematic model of α and γ iPP branching from α 'parent' lamellae. The crystallographic axes are indicated. Adapted from similar schemes in Refs. [17,22].

and with mol% ethylene varying from 0.8–4.6% were studied. Details of their molecular characterizations are given in Table 1. Besides the structural irregularity introduced in the chain by the comonomer, the samples have a similar mole fraction of defects introduced by tacticity (0.70±0.13)% and very similar mole fraction of misinsertions of the 2,1 erythro type (0.42±0.07)%. The sum of the concentrations of all types of defects is also listed in the table. A homopolymer (M180K1.60) synthesized with the same catalyst under the same experimental conditions was also studied. It displays the same content of stereo-irregularities as the copolymers and double the amount of regio defects. The total defect concentration, 1.6 mol%, is similar to the lowest defected copolymer and enables comparison of the types of defects on the growth rates.

The molecular masses and molecular mass distributions are very similar for these copolymers. Therefore, the effect of molecular mass and concentration of stereo and regio defects on the crystallization can be considered constant, and differences in the linear growth rates among the copolymers will reflect the effect of increasing ethylene content on the crystallization kinetics. The same set of copolymers has been used in previous studies of their polymorphic behavior [13] and spherulitic and lamellar morphologies developed by these materials [14].

The molecular masses and their distributions were determined by standard gel permeation chromatography using polystyrene standards for calibration. The type and fractional content of all the defects was obtained by solution $^{13}$C NMR as previously detailed [15,26–29].

### 2.2. Polymorphic analysis

The temporal evolution of the fractional content of α and γ crystals at a constant crystallization temperature was followed from the heat of fusion of the dual meltings obtained by differential scanning calorimetry. As demonstrated in a previous work the endotherms corresponds to α crystals, the uppermost melting peak and to the melting of γ crystals the lowest temperature melting peak [13,16]. Each copolymer was initially melted at 200 °C for 3 min and cooled at a rate of 40 °C/min to the required crystallization temperature. After a given time had elapsed, the partially crystallized copolymer was melted at 10 °C/min starting from the crystallization temperature. The crystallization was repeated for increasing elapsed times until the increase in heat of fusion from successive endotherms was negligible or after unduly long times for crystallization were required. The areas of each α and γ melting peaks were manually deconvoluted.

The evolution of both polymorphs was also followed by WAXS obtained at the isothermal crystallization

Table 1
Molecular characterization of metallocene homopolymer and metallocene propylene ethylene copolymers

| Sample | Comonomer type | Comonomer (mol%) | Regio (mol%) | Stereo (mol%) | Total defects (mol%) | $M_w$ (g/mol) | $M_w/M_n$ |
|---|---|---|---|---|---|---|---|
| M180K1.60 | – | 0.0 | 0.8 | 0.8 | 1.6 | 180,000 | 1.90 |
| PE1.8 | Ethylene | 0.8 | 0.4 | 0.6 | 1.8 | 233,100 | 1.98 |
| PE2.8 | Ethylene | 1.7 | 0.4 | 0.7 | 2.8 | 221,300 | 1.81 |
| PE3.4 | Ethylene | 2.2 | 0.5 | 0.7 | 3.4 | 214,800 | 1.75 |
| PE5.8 | Ethylene | 4.6 | 0.4 | 0.8 | 5.8 | 251,000 | 2.12 |

temperature in selected copolymers. Diffraction patterns were collected using a Siemens D500 diffractometer with an attached Anton Paar HTK high temperature head. The instrument was calibrated for d spacing with standard polycrystalline quartz and for temperature with recrystallized benzil (diphenylethanedione, mp = 95.0 °C). The diffraction peak assignments for the α and γ phases followed those given by Bruckner and Meille [21] and Turner Jones [30] and the α and γ indexes were quantified from the heights of the (1 1 7) γ reflection at $2\theta = 20.1°$ and the (1 3 0) α reflection at $2\theta = 18.8°$, after subtracting the amorphous background. The fractional content of γ crystals was obtained as $H_\gamma/(H_\gamma + H_\alpha)$.

### 2.3. Linear growth rates

Linear growth rates were measured in $40 \pm 10$ μm thick films using an Olympus BH-2 optical microscope fitted with an Olympus DP/2 digital camera and a Linkam hot stage TP-93. The temperature was controlled with a precision of ±0.1 °C. The film was placed between two microscope cover slips and heated to 200 °C for 5 min to eliminate any crystalline memory. Subsequently the temperature was lowered at a rate of 40 °C/min to the crystallization temperature. The complete crystallization process was recorded on a videotape and the diameter of the spherulites measured as a function of time, till impingement. Linear growth rates ($G$) were obtained from the average of the linear plots of the spherulite radius versus time. At least three spherulites per view area were measured for each crystallization temperature. Following this method $G$ values were obtained with uncertainties of $\pm 0.01 \times 10^{-6}$ cm/s.

AFM images were obtained using the environmental Jeol 4210 scanning probe microscope operating under ambient conditions. Topographic and phase images were simultaneously collected in non-contact AC mode at 256×256 standard resolution using Olympus single side coated silicon cantilevers with resonant frequency at ~300 kHz.

## 3. Results and discussion

The simultaneous isothermal development of the α and γ polymorphs were followed by DSC, and also by WAXS in selected samples, as described in Section 2 and in our previous work [13]. Representative WAXS patterns of copolymer PE3.4 during crystallization at 115 °C are given in Fig. 2(a) for different crystallization times. Diffraction peaks characteristic of the α and γ phases are observed at the earliest detection of crystallinity, a feature characteristic of their intimate association through their epitaxial interaction. Shortly after 50 min the intensity of the α reflection remains constant while the γ increases and levels off after about 120 min. Parallel melting curves after crystallization in the DSC are shown in Fig. 2(b). They confirm, by the difference in melting behavior, the dynamic

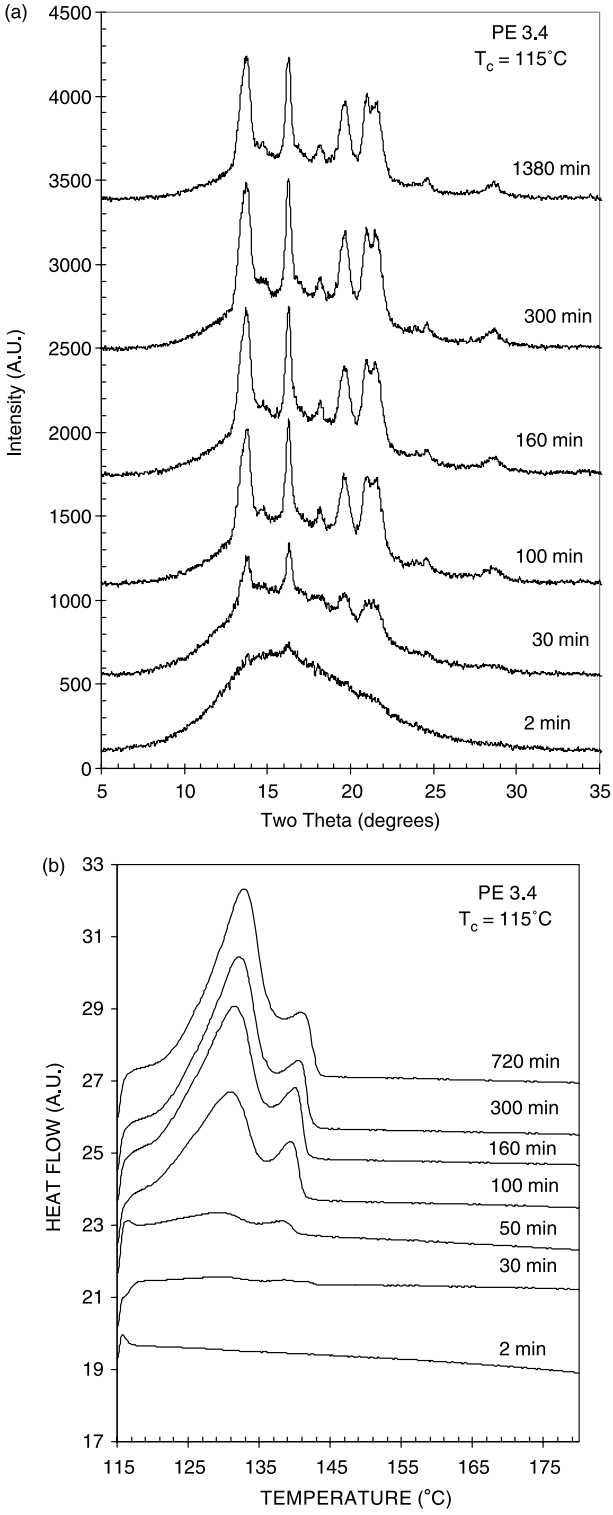


Fig. 2. (a) WAXS diffractograms of PE 3.4 obtained during crystallization at 115 °C at the times indicated. (b) DSC melting started from the crystallization temperature.

change in the content of both types of crystals during isothermal crystallization, and correlate closely with the X-ray data. The area of the high-temperature melting peak, corresponding to the alpha crystallinity, becomes constant

after ~50 min. while the lower melting peak, associated with γ crystallinity continues to increase and levels off at much longer times. Hence, WAXS or DSC data allow independent analysis of the development of both types of crystals.

The evolution with time of the heat of fusion corresponding to each polymorph is shown for selected crystallization temperatures ($T_c$) for all copolymers in Fig. 3(a)–(d). These figures give quantitative data of the α and γ crystallinities developed with time during isothermal crystallization. In all copolymers, at any $T_c$, both polymorphs are formed simultaneously from the early stages of the crystallization and both evolve with the typical sigmoidal behavior. For all copolymers α crystallinity, represented by the closed symbols in Fig. 3, quickly reaches a constant value that decreases with increasing $T_c$. Conversely, the γ crystallinity only levels off at the lowest $T_c$s and continues to increase with time at higher $T_c$s. Upon final transformation, γ crystallinity first increases with $T_c$, reaches a maximum value and then decreases slightly with further increase in $T_c$. As a consequence, the fractional crystal content in γ phase increases rapidly with increasing $T_c$ in any of the copolymers studied [13]. These features are important to correlate the relative content of both types of crystals with measurements of the spherulitic growth rates. The evolution of the heat of fusion shown in Fig. 3 indicates that at any of the experimentally accessible $T_c$s, there is an interval of time for which crystallization proceeds exclusively via the formation and growth of γ crystallites, the region where α levels off and γ continuous to grow. Thus, Fig. 3(a)–(d) enable time frames in the crystallization process to isolate the behavior of the γ phase from the crystallization of mixed α+γ phases. An additional important feature to notice is the dominance of γ crystallinity from the early stages of the crystallization at the highest $T_c$s. The question to address from these data is if the linear growth rate changes when growth of α crystallites stops, as inferred by the simultaneous α−γ branching structural model of Fig. 1.

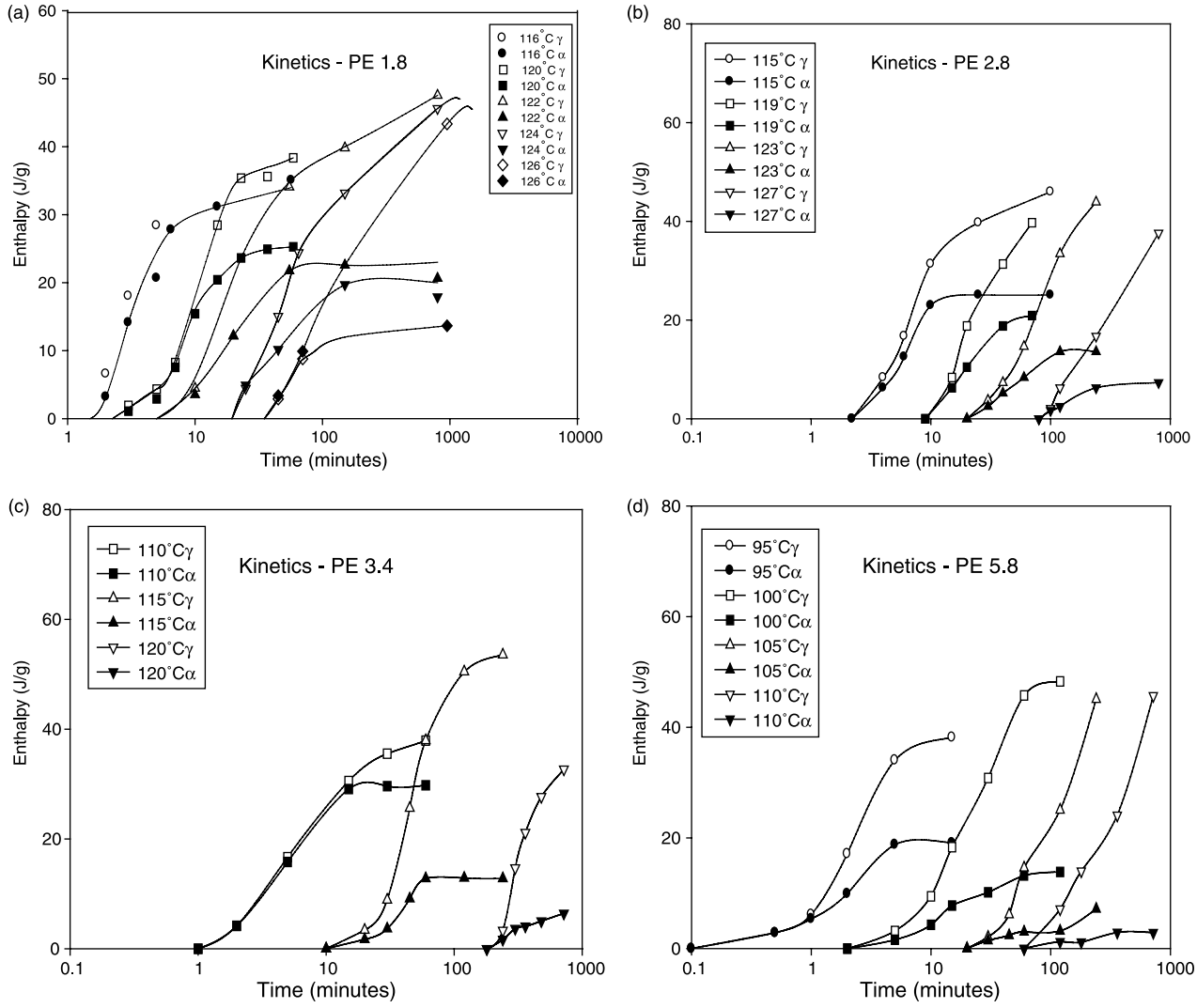


Fig. 3. Sigmoidal development of α (filled symbols) and γ (open symbols) crystallinities with time at the indicated temperatures for copolymers: (a) PE 1.8, (b) PE 2.8, (c) PE 3.4, (d) PE 5.8.

The crystallization of pure γ crystallites can be monitored by extending the measurements of the spherulitic radius with time to the region where pure gamma form prevails, i.e. the flat region of the α sigmoidal curve. This is not experimentally feasible at the lowest isothermal $T_c$s because the spherulites impinge before the content of alpha phase levels off, as seen in the optical micrograph of Fig. 4(a) for PE 2.8 crystallized at 120 °C for 20 min. At these low $T_c$s the gradient of the radius with time is measured in the time regime of mixed α+γ crystallization. At higher $T_c$s the nucleation density decreases and the spherulitic growth can be followed up to the region of pure or predominantly γ growth before impingement, as shown in the micrograph of Fig. 4(b). Here the linear growth of the spherulites of the same copolymer crystallized at 127 °C could be followed for times in which the crystallization proceeds as pure γ crystals. Any differences in the spherulitic growth between the regions of mixed α and γ growth and pure γ growth are only to be observed in the high $T_c$ regions. Representative data of the change in spherulitic radius with time for copolymer PE 2.8 are given in Fig. 5 for $T_c$s spaced 1 °C in the interval between 118 and 131 °C. Clearly a sharp break in the linear growth with time is observed for all $T_c$s ≥ 127 °C. It should be noted that this is the $T_c$ region where spherulitic growth could be experimentally followed for predominantly or pure γ growth. To test if the observed break in growth is a consequence of truncation of spherulites present within the relatively thin (∼40 μm) film, measurements in the high $T_c$ range were repeated using 150 μm films. A similar sharp break was observed independent of film thickness.

A second concern in reference to non linearity of spherulitic growth relates to the copolymeric nature of these materials and to the fact that the ethylene co-unit is partially discriminated against entering the crystalline regions [15]. As a consequence, the concentration of ethylene in the melt of the growing crystallite increases during transformation. The continuous increase with time of co-unit content in the melt should be reflected in a continuous decrease in the rate of growth during the isothermal transformation. However, what is observed is a sharp break between two growth domains at temperatures and time frames that correlate to the simultaneous growth of mixed α and γ polymorphs at the early stages and with the growth of pure gamma crystallites at a later stage in the transformation. Similar sharp breaks were observed while measuring the spherulitic growth of PE 1.8 for $T_c \geq 129$ °C. It is, thus, quite evident that the liquid–solid transformation to pure gamma phase proceeds with significantly lower linear growth rates than those corresponding to the formation and growth of mixed polymorphic forms. At high $T_c$s the spherulites of the two ethylene rich copolymers become irregular with time and the change in slope could not be obtained.

Fig. 6 displays the natural logarithm of the linear growth rate of PE2.8 versus $T_c$. The experimental $G$ values in the region of mixed α+γ growth are given by the slopes at the earlier growth times in Fig. 5. These data are plotted as closed symbols in Fig. 6. They represent the growth of α lamellae ($G_\alpha$) according to the dictates of the structural models for γ branching from α surfaces given in Fig. 1. The data for transformation to pure gamma phase are also included as open symbols ($G_\gamma$). With increasing $T_c$ the growth rate is reduced by a factor of 30 in the 13° range analyzed, indicative of a large negative temperature coefficient of the rate, which is typical of nucleation controlled processes. In addition, the $G(\alpha)$ data presents a discontinuity in the temperature gradient at the change over between γ dominated growth and α+γ mixed growth. Hence, it appears that the dominance of γ growth during crystallization affects $G(\alpha)$ compared to the behavior when both polymorphs develop at about the same content. To the best of our knowledge this is the first time that the discontinuity in the kinetics of linear growth of propylene copolymers has been directly correlated with a change in polymorphic growth.

It was reported long ago that interruptions in the regular sequence of isotactic poly(propylene) favour the development of the γ polymorph [23]. As there is discrimination against the ethylene co-unit from entering the crystal,

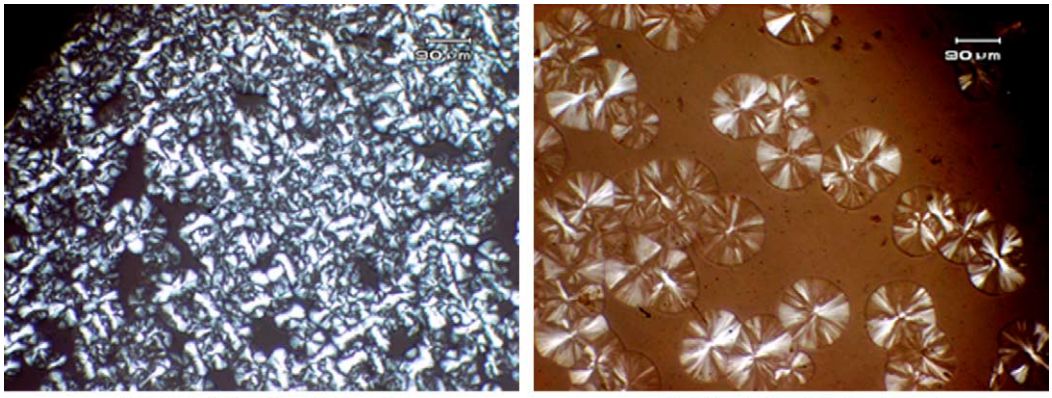


(a) PE 2.8 T= 120 °C, 20 min. (b) PE 2.8 T= 127 °C, 150 min.

Fig. 4. Polarized optical micrographs for PE 2.8 obtained at $T_c$s and times indicated.

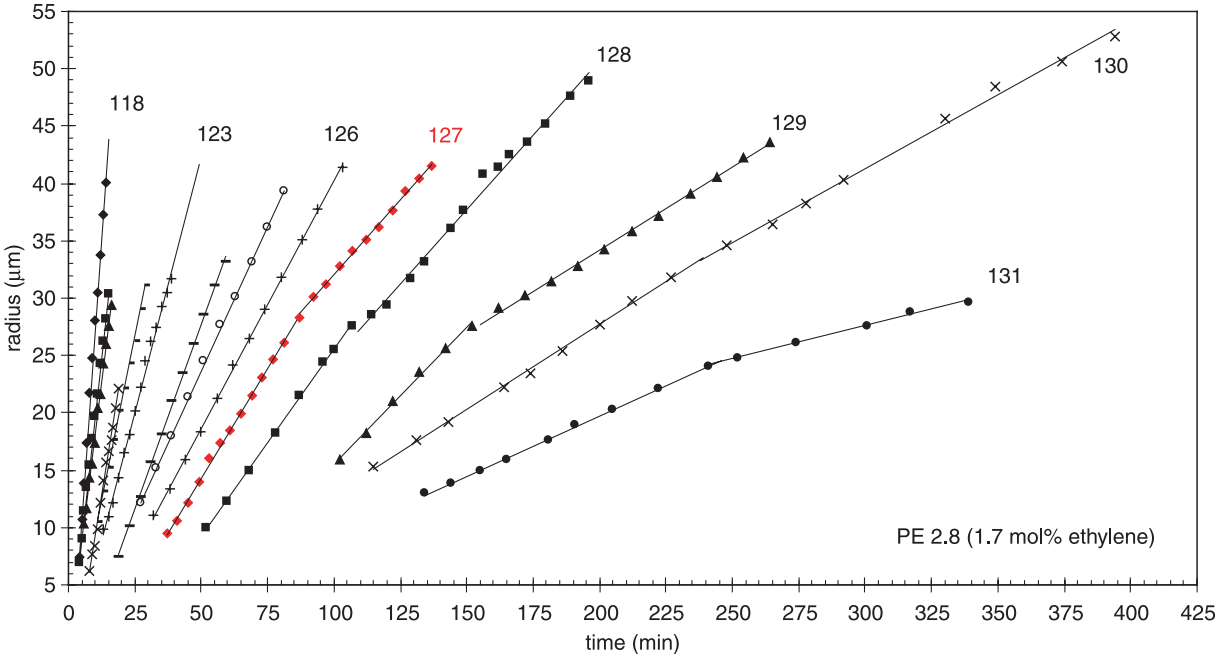


Fig. 5. Spherulitic radius vs. time for PE 2.8 at the indicated $T_c$s. The data display two rates of growth for $T_c$s > 126 °C.

increasing the concentration of ethylene in the chain decreases the length of isotactic sequences paralleling the increased development of crystals in γ form. The requirements for short isotactic sequences in the chain added to stem length requirements to form stable crystallites at the low undercoolings where the γ polymorph prevails [30], suggests a crystallization for this polymorph based on selecting full length sequences. In other words, it follows a type of 'extended sequence' crystallization. Added to the peculiarities of its crystallographic registry, it has been proposed that γ crystallites grow by staggering these crystallizable sequences with a reduced importance for chain folding [22,32,33]. Henceforth, the discontinuity in the temperature gradient of the linear growth rates is identified with the changeover from an extended-like crystallization mechanism at high temperatures, where γ dominates, to a folded type crystallization mechanism at temperatures where α and γ crystallize with similar contents. This transition parallels the behavior observed in low molecular weight polyethylene oxides [34,35], low molecular weight polyethylenes [36,37], and long-chain *n*-alkanes [38,39], that undergo a similar extended to folded type change in crystallization mechanisms with increasing undercooling.

The experimental observations, given in Figs. 5 and 6 also display linear growth rates for pure γ phase significantly lower than those that correspond to mixed α+γ development. On the basis of these data it is concluded that the growth of pure γ is lower than the growth of α phase ($G\gamma < G\alpha$). They confirm earlier

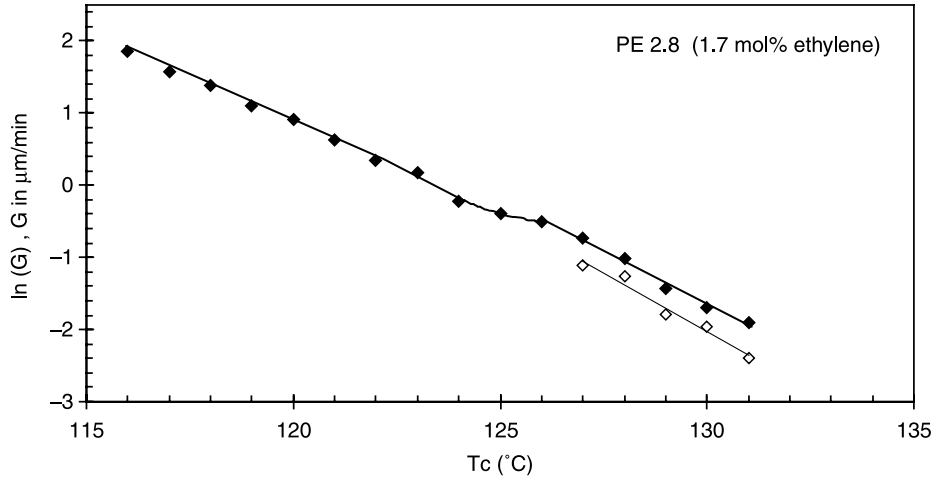


Fig. 6. Logarithm of the growth rate ($G$) vs. crystallization temperature for PE 2.8. Filled symbols: α growth, open symbols: γ growth.

suggestions by Meille et al. [32] about limitations posed by the existence of non-parallel chain orientations in the crystallographic registry of the γ phase on the possible growth mechanisms of this polymorph. Compared to parallel chain crystallites of the α and β iPP polymorphs, for which the above constraints should not apply, there was speculation that the growth of γ-iPP crystals should be kinetically disfavored. The experimental $G$ data of the copolymers are in line with the speculated kinetic restrictions, and are also in line with expectations of a change in spherulitic growth habits at the time when α radial growth is discontinued, as indicated by the growth model of Fig. 1.

The spherulitic regions of pure γ growth were imaged by AFM to contrast their lamellar habits with characteristic features corresponding to mixed polymorphic growth. The images obtained in a PE2.8 specimen crystallized at 130 °C for 450 min and further quenched at room temperature are given in Fig. 7. As observed in the optical micrograph, the spherulites display a lack of any noticeable change in birefringence before and after the break in growth rates. AFM images of regions of pure γ growth are shown in this figure at three different magnifications. The observed dense parallel arrays of short lamellae, oriented transverse to the spherulite radius, conform with the characteristic morphologies of γ-rich copolymers discussed in our previous work [14]. Although there is no α development in this region, the observed orientation of γ lamellae follows that expected for γ crystals branching from radially oriented α surfaces. Long and thicker lamellae, oriented in the direction of the spherulitic radius and associated with the α phase, are observed nearer the spherulitic origin, as previously evidenced [14], but are not apparent in the peripheral spherulitic regions shown in Fig. 7. It is then concluded that prior to the break in Fig. 5, the measurement of spherulitic diameter is led by the radially oriented α growth, while after the break spherulitic growth appears to proceed by the formation of new gamma lamellae and not by the direction of their preferred growth, the $c$ axis of the non-parallel chain γ structure [21]. The origin for the specific orientation of γ crystals, in the absence of α growth, is unknown. It is possible that orientational order of the alpha structure may continue to increase with insignificant changes in the heat of fusion or in the X-ray diffraction peak characteristic of the alpha phase. This order could provide hidden α seeds, difficult to detect, that direct the orientation of γ lamellae outgrowing from them, according to the model of Fig. 1 [14]. Moreover, if indeed some sort of α surface is leading the radial spherulitic growth, the experimental measurement before and after break will correspond to the α form notwithstanding a crystallization mode, after the break, totally dominated by the gamma phase. This appears unlikely and, in this respect we point out that orientational order or hidden seeds could also be of a γ nature, since γ branching from both α or γ surfaces appears feasible [22].

The linear growth rates of the homopolymer and the four copolymers studied are given in Fig. 8 as a function of crystallization temperature. The $G$ data in the region of pure γ growth have been omitted for clarity in the presentation. Hence, the data in this figure represent $G$ of the α phase corresponding to $T_c$ domains of simultaneous α+γ growth (low $T_c$) and domains where the content of γ is much higher than α (high $T_c$s). The growth rates decrease sharply with increasing $T_c$ and their displacement along the $T_c$ axis with increasing ethylene, reflects the drastic influence of co-unit content on the crystallization rate for a fixed molecular weight. The shapes of the curves, characteristic of the temperature gradient of the growth rate of the copolymers, are all very similar. Analogous to the behavior of random ethylene copolymers [31], the growth rates do not fall on the same curve when plotted vs. undercooling, instead of $T_c$. We find from Fig. 8 that in order to maintain a given growth rate, a substantial increase in undercooling is required as the co-unit content increases. For example using the $T^{\circ}_{m\ copo}$ calculated in the following section, a $G=2.72$ μm/min requires a $\Delta T$ of 61 °C for PE1.8 (0.8 mol% ethylene) while a $\Delta T$ of 74 °C is necessary for the copolymer PE 5.8 (4.6 mol% ethylene) to maintain the same rate. Conversely, at a fixed undercooling, the crystallization rate decreases drastically with increasing co-unit content. Of special interest in Fig. 8 is that all the growth rates curves of the copolymers studied display a discontinuity at $T_c$s where the γ phase becomes the dominant structure from the early stages of the crystallization. Discontinuities in the temperature gradient, shown by arrows in the figure, occur at ~129 °C for PE1.8, at ~126 °C for PE2.8, at 119 °C for PE3.4 and ~107 °C for PE5.8. By comparison with the overall crystallization of both forms shown in Fig. 3, it is clear that α crystallites develop in very small contents at and above these $T_c$s. A general behavior is thus observed for the linear growth rates of random polypropylene ethylene copolymers. The change in mechanism from crystallization of extended sequences (high $T_c$ domain) to folded chain crystallization (low $T_c$s), leads to a break in the temperature gradient of their growth rates.

The data of the homopolymer are added in Fig. 8 as a test of the correspondence in copolymers between the discontinuity in the gradient of the rate and the change to preferential γ growth. Lack of comonomer and a slightly lower concentration of defects in the homopolymer, compared to the least defected PE1.8 copolymer, lead to slightly higher $G$ values. In addition, the experimental range of $G$ measurements in the homopolymer is extended to much higher $T_c$s. Thus, while at 135 °C the crystallinity of PE1.8 becomes too low for reliable $G$ measurements, the spherulitic growth of the homopolymer could be followed up to 144 °C. Discontinuities in the temperature gradient are not observed in the homopolymer. Lack of a break similar to that found in copolymers is explained by the nature of the isothermal development of α and γ crystallinities with time in the $T_c$ range where the growth rates of the homopolymer can be experimentally followed. The data for the

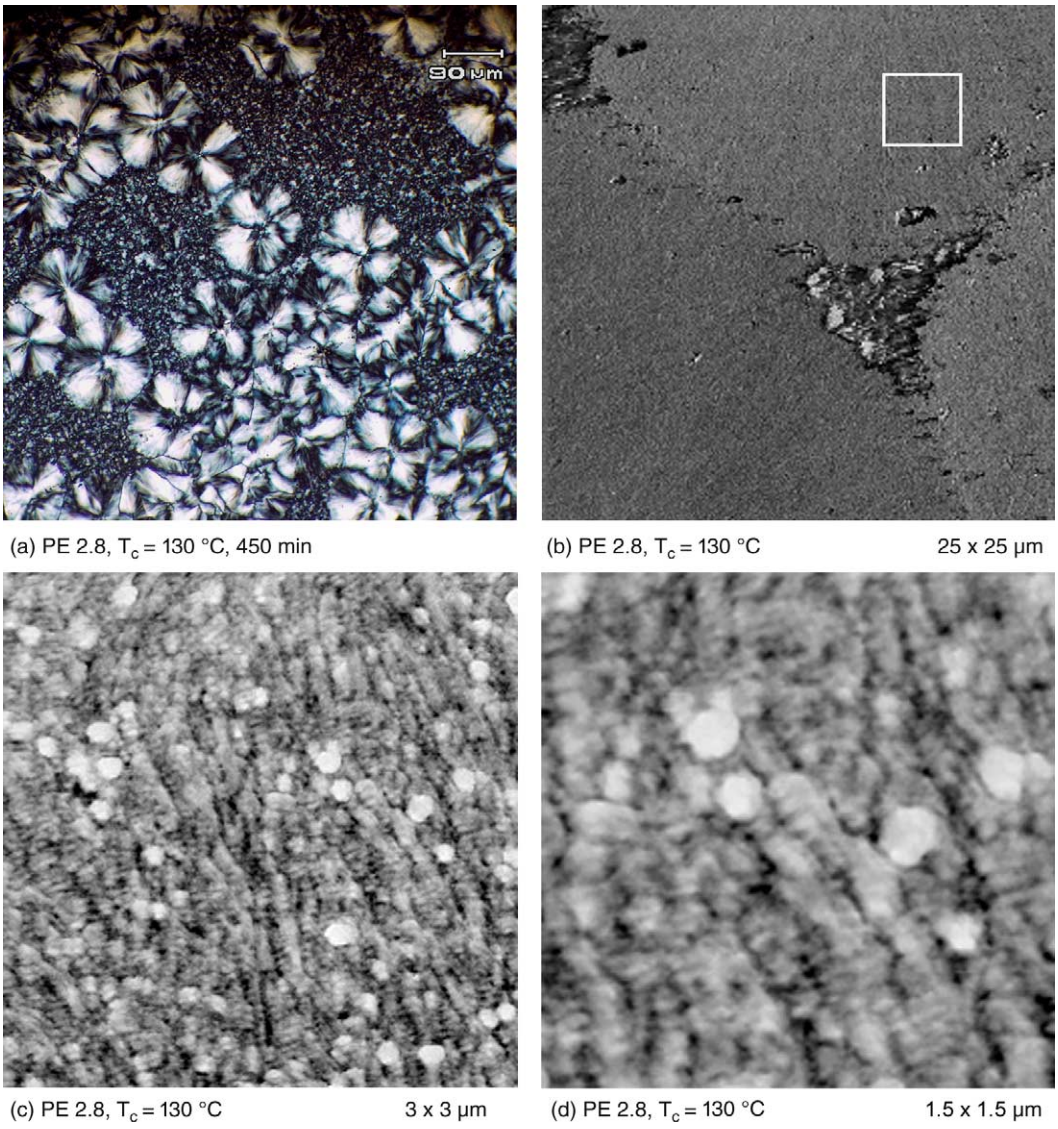


Fig. 7. Spherulitic and lamellar morphologies of PE 2.8 crystallized at 130 °C for 450 min and further quenched at room temperature. (a) Polarized optical micrograph. (b) 25×25 µm$^2$ AFM phase image. White square indicates the region of pure γ growth where higher resolution AFM images where taken. (c) 3×3 µm$^2$ AFM phase image of the spherulitic region of pure γ growth. (d) 1.5×1.5 µm$^2$ AFM phase image of the same region.

development of α and γ crystallinities for the homopolymer were given in a previous work (see Fig. 15 of Ref. [16]). The initial crystallization times of both polymorphs were found to be the same at each crystallization temperature, analogous to the copolymer behavior. However, for this homopolymer, the content of γ crystals (γ crystallinity) never becomes dominant in the range of temperatures and times where the spherulitic growth can be measured. For $T_c$s below 125 °C both polymorphs develop with the same fractional content, in the $T_c$ range between 125 and 133 °C although the concentration of α crystals levels off and γ continue to crystallize, the spherulites impinge well before γ crystallinity overcomes the value for α, therefore, $G$ for γ growth cannot be measured. In the high $T_c$ range, above 133 °C, the crystallization proceeds with equal contents of α and γ phases or is dominated by the α phase. A change from mixed γ+α crystals to preferential growth of γ crystallites does not occur in the homopolymer; as a consequence, the growth rates of the homopolymer display a continuous gradient in the whole $T_c$ interval. Hence, as mentioned earlier, the $G$ data of the homopolymer are indirect evidence for the change in growth mechanism observed in the copolymers.

The spherulitic growth rates of a series of fractions obtained from a ZN iPP displayed multiple discontinuities with increasing temperature [40]. One of the breaks in $G$ was associated with the transition from regime II to III according to Hoffman's growth regimes theory [41–44]. In order to test a possible overlap between the changeover from extended-type to folded crystallization with a change in growth regime, the experimental $G(\alpha)$ data of the copolymers was analyzed according to secondary nucleation theory [41–44].

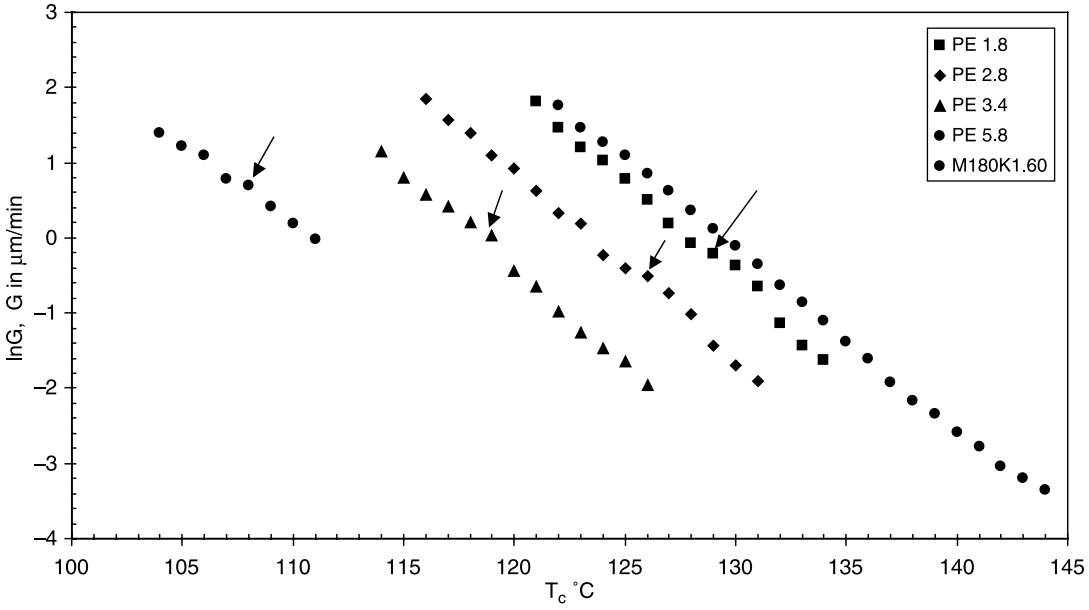


Fig. 8. Logarithm of α growth rate ($G$) vs. crystallization temperature for metallocene homopolymer and propylene ethylene copolymers indicated. The arrows indicate the discontinuity in the temperature gradient of the growth rate of the copolymers.

Lauritzen and Hoffman adapted earlier developments by Hillig [45] and other authors [46,47] for metals and monomeric species to the polymeric growth. The growth process of polymeric lamellae was envisioned as successive nucleation and spreading events over a crystal surface, initially generated by the primary nuclei. The net growth rate ($G$), perpendicular to the crystal face, depends on the relative values of the surface or secondary nucleation rate ($i$) and the rate of spreading or lateral growth rate ($g$). The relative values of $i$ and $g$ change with undercooling and lead to a different dependence of the overall $G$ rate with $i$ and, thus, to different crystallization regimes [41–44]. Namely, at low undercoolings, the nucleation rate is very small compared to the rate of spreading ($i \ll g$), a single nucleus spreads and completes a layer before a new nucleus is formed. Thus, each surface nucleation act results in the addition of a new surface layer. The overall $G$ is nucleation controlled, $G$ is proportional to $i$, and the $T_c$ interval where this mechanism is operative is termed regime I [42]. As the undercooling increases, the rate of surface nucleation increases and becomes comparable to $g$. Multiple nucleation events are allowed to occur on the surface before layer spreading is completed. Now $G$ is proportional to $(ig)^{1/2}$ and corresponds to regime II [42]. At very large undercoolings excessive surface nucleation leads to effectively zero spreading rates and the overall $G$ is again proportional to $i$ [43,44]. This low $T_c$ range corresponds to regime III. The temperature coefficient of the growth rate in this regime has the same functionality as that of regime I.

In general, the overall growth rate of a polymeric crystal can be described by the equation: [41,42]

$$G = G_0 \exp\left[\frac{-U^*}{R(T_c - T_\infty)}\right] \exp\left[\frac{-K_g}{T_c \Delta T f}\right] \quad (1)$$

The pre-exponential term $G_0$ involves all the terms weekly dependent on temperature, $U^*/R(T_c - T_\infty)$ is the term associated with segmental transport across the crystal–liquid interface. It is formulated taking the Vogel–Fulcher–Tamman–Hesse expression to describe the effective activation energy for segmental transport in the crystallization process [48–50]. $T_\infty$ represents the temperature below which the required segmental motion becomes infinitely slow. It is usually taken 30–50 K below $T_g$ ($T_\infty = T_g - C_2$). The values of $U^*$ and $T_\infty$ of most semicrystalline polymers are unknown. Two sets of values, $U^* = 4120$ cal/mol, $C_2 = 51.6°$ and $U^* = 1500$ cal/mol and $C_2 = 30°$ were treated as universal [42]. However, it was later pointed out that the $U^*$ and $C_2$ constants should be used as adjustable parameters to enable gradients of the temperature coefficient of the rate conforming to crystallization regimes [51–55].

The nucleation term, $K_g/(T_c \Delta T f)$, is the effective energy barrier to form a stable critical nucleus on the pre-existing surface. $\Delta T$ is the undercooling $(T_m^\circ - T_c)$, $f = 2T_c/(T_m^\circ + T_c)$ is a correction factor to include higher order terms of the variation of the heat of fusion with temperature and $K_g$ is expressed as: [42]

$$K_g = \frac{Y b_0 \sigma \sigma_e T_m^\circ}{k \Delta H_u} \quad (2)$$

with $Y = 2$ for Regime II and $Y = 4$ for Regimes I and III. $b_0$ is the stem or layer thickness, $k$ the Boltzmann's constant,

$\Delta H_u$ the heat of fusion, $\sigma$ and $\sigma_e$ the lateral and fold surface free energies of the nucleus that evolves and $T_m^\circ$ the equilibrium melting temperature.

Analysis of growth rate data obtained for homopoly (propylenes) and fractions from the homopolymer, according to Eq. (1), had invariably led to breaks consistent with a Regime III–II transition in the mechanism of growth [40, 54–56]. Occasionally, data at low undercoolings and for iPP fractions of low molecular mass appear to display a II–I regime transition in addition to the III–II transition most generally found [40,57]. In contrast, the growth rate data of random propylene ethylene copolymers available in the literature have usually been obtained in too narrow temperature ranges to display any possible change in crystallization regimes [2–4]. Only in one instance [1], a III–II transition was clearly indicated for an unfractionated ZN propylene ethylene copolymer, but the heterogeneous nature of the distribution of comonomer and broad molecular weight distribution precludes conclusions in terms of any correlation between the observed regime transition and the polymorphic issues raised in the present work. The analysis of the temperature coefficient of the linear growth rates obtained here for metallocene propylene ethylene copolymers, according to Eq. (1), requires knowledge of the equilibrium melting temperature of each copolymer. The determination of these values is discussed in the Section 3.1.

### *3.1. Equilibrium melting temperatures of propylene ethylene random copolymers*

Direct evidence of ethylene inclusion in the crystal lattice for these copolymers was obtained by cp MAS $^{13}C$ NMR studies [15]. The concentration of ethene units in the crystal ($X_c$) was determined from the NMR spectra corresponding to the crystalline regions and are listed in Table 2 for copolymers with ethylene content ($X_B$) changing from 0.8 to 7.5 mol%. $X_c$ was found to scale linearly with the overall concentration of ethylene in the chain. Moreover, the values of $X_c$ are much lower than those of $X_B$ indicating much lower concentrations of ethylene in the crystal than the ethylene chain concentration. $X_c$ is also lower than the concentration of ethylene in the non-crystalline regions. In other words, during crystallization there is discrimination against the ethylene co-units from entering the crystal. The ethylene content is not equally distributed between the crystalline and non crystalline regions precluding the use of any thermodynamic models that assume either total exclusion of the ethylene unit from the crystal or models with uniform distribution of the co-unit.

Table 2
Data related to ethylene concentrations, overall ethylene concentration in the copolymer ($X_B$), ethylene concentration in the crystalline regions ($X_c$), excess energy per mole of ethylene incorporated in the crystal ($\varepsilon$), and equilibrium melting temperatures of the alpha ($T_{m\ copo}^\circ$)($\alpha$), and of the gamma ($T_{m\ copo}^\circ$)($\gamma$), crystals for propylene ethylene copolymers

| $X_B$[a] (mole fraction) | $Xc$[b] (mole fraction) | $\varepsilon$[c] (kJ/mol) | ($T_{m\ copo}^\circ$)($\alpha$) (K) | ($T_{m\ copo}^\circ$)($\gamma$) (K) |
|---|---|---|---|---|
| 0.008 | 0.00336 | 2.90 | 458.2 | 459.2 |
| 0.017 | 0.00714 | 2.92 | 457.1 | 458.0 |
| 0.022 | 0.00924 | 2.93 | 456.5 | 457.3 |
| 0.0459 | 0.0193 | 2.97 | 453.7 | 454.2 |
| 0.0747 | 0.0314 | 3.0 | 450.2 | 450.4 |

[a] Moles of ethylene per mole of monomer units.
[b] Moles of ethylene per mole of crystalline repeat units.
[c] Average $\varepsilon$ value for propylene ethylene copolymers: $2.94 \pm 0.05$ kJ/mol.

Thermodynamic treatments to obtain equilibrium melting of statistical (random) copolymers have been recently reviewed by Crist [58]. Of concern to the present work is the Sanchez–Eby (SE) [59,60] treatment that considers the case of co-units included as defects in the crystals,[1] and, thus, is appropriate to the propylene ethylene copolymers of interest in this work, in reference to the NMR results. In the limit of infinite crystal thickness, the melting temperature of copolymer crystallites ($T_{m\ copo}^\circ$) with crystal composition $X_c$, in equilibrium with a melt of composition $X_B$ (the overall chain composition) is given by the following equation: [59, 60]

$$\frac{1}{T_m^\circ} - \frac{1}{T_{m\ copo}^\circ} = -\frac{R}{\Delta H_u}\left[\varepsilon\frac{X_c}{RT_m} + (1-X_c)\ln\left[\frac{(1-X_c)}{(1-X_B)}\right] + X_c\ln\left[\frac{X_c}{X_B}\right]\right] \quad (3)$$

$T_m^\circ$ is the equilibrium melting temperature of the ethylene free homopolymer crystals and $\varepsilon$ the excess free energy per mole of ethylene unit incorporated in the crystal. The value of $T_m^\circ$ for the homopolymer has been controversial for decades and still is an unresolved issue [55,62–64]. Values in the range of 212–186 °C have been reported. In analyzing thermodynamic properties for the homopolymer, the iPP chain should be considered as a copolymer because stereo or constitutional chain defects, generated during synthesis, are for all practical effects co-units that could be either rejected or partially included in the crystalline regions [69]. Hence, by definition, the equilibrium melting temperature of the homopolymer is the melting temperature of the thickest (thickness $\rightarrow \infty$) crystals coexisting with a melt of composition corresponding to the overall defect composition of the chain ($X_B$).

Because of the copolymeric nature of iPP, some precautions are needed, as detailed by Crist [58], when using thermal data in the usual extrapolations leading to $T_m^\circ$ to ensure that the observed melting temperatures correspond to crystallites coexisting with melts of composition $X_B$.

[1] The S–E treatment has received some criticism because the formulation of the partition function did not account for the sequence distribution in the crystalline regions [61].

Extrapolations based on the Gibbs–Thompson equation should be carried out with experimental data for thickness and melting temperatures obtained at very low levels of crystallinity because only for the incipient crystallites is the composition of the melt the closest to the chain composition. In addition, experimental conditions need to be chosen to minimize isothermal melting kinetics [70]. Crist [58] also showed that the so-called Hoffman-Weeks extrapolation always underestimates the true equilibrium melting temperature of statistical copolymers. The idea is the following: melting of the thickest crystals is never observed because the concentration of long sequences available to form these crystallites is extraordinarily small. Then, any $T_m/T_c$ extrapolation, even if carried out with data corresponding to the final melting trace when levels of crystallinity are minimized, will lead to the largest observable meting temperature and not to that corresponding to the very thick crystals that form from the small fraction of sequences of the longest possible length.

In two recent studies that use the Hoffman-Weeks extrapolation to obtain $T_m^\circ$ of iPP, the need to use low levels of crystallinity was acknowledged and isothermal crystal thickening and superheating effects were taken into account, however, the copolymeric nature of the chain was ignored [55,62]. Therefore, the extrapolated $T_m^\circ$ values correlate with the thickest crystallite observable and differ from the true $T_m^\circ$. In the works of Mezhgani and Phillips [64,65], both Hoffman–Weeks and Gibbs–Thompson extrapolations were adapted to obtain thermodynamic data of the α and γ iPP forms. However, the low crystallinity requirement when using the Gibbs Thompson approach was not met in these works.

We then face a situation of lack of a sounded thermodynamic $T_m^\circ$ value for the homopolymer. However, while we acknowledge the shortcomings of the available $T_m^\circ$ values, we find that the main conclusions from the kinetic analysis of PE copolymers, discussed in next section, are unchanged by the choice of $T_m^\circ$ in the interval of 220–185 °C. In the interest of carrying out independent kinetic analysis for α and γ growths in the series of PE copolymers analyzed in this work, calculations of $T_{m\ copo}^\circ$ were performed according to Eq. (3) using the $T_m^\circ$ values given by Mezghani and Phillips [65] for both polymorphs. The following two sets of data were given in this work:

$T_m^\circ(\alpha) = 186.1$ °C, $\Delta H_u\ (\alpha) = 209$ J/g and $T_m^\circ(\gamma) = 187.2$ °C , $\Delta H_u\ (\gamma) = 190$ J/g.[2]

These and other material parameters characteristics of the α and γ iPP polymorphs, used in the analysis of the temperature coefficient of the growth rates, are listed in Table 3.

The value of $\varepsilon$ can be found considering that $X_c$ reaches some equilibrium value ($X_c^{eq}$) [59]. For the copolymers of interest in this work, additional NMR data [15], and indirect melting studies to be reported in a forthcoming publication [71], indicate that $X_c$ is basically constant with crystallization temperature. On this basis, $X_c^{eq}$ takes the $X_c$ value of a given propylene ethylene copolymer, and $\varepsilon$ is found from the following relation: [59]

$$X_c^{eq} = \frac{X_B e^{-\varepsilon/RT_m}}{1 - X_B + X_B e^{-\varepsilon/RT_m}} \quad (4)$$

$\varepsilon$ and $T_{m\ copo}^\circ$ values calculated for the alpha and gamma crystals are listed in Table 2[3]. In the range of ethylene concentration studied, the equilibrium melting temperatures, calculated according to Eq. 3, differ among the copolymers by 8°.

An average $\varepsilon$ of $2.94 \pm 0.05$ kJ/mol was found for all copolymers independently of concentration of ethylene. This value is similar to the 2.45 kJ/mol given for L and DL lactides [72] and is similar to values found for other systems in which the defect does not involve a different chemical repeat unit. Since the ethylene unit does not disrupt the 3/1 helical registry of the poly(propylene) chain, it appears that the accommodation of some ethylene units in the poly(propylene) crystal lattice does not pose a too large free energy excess.

The heat of fusion per mole of crystalline units of propylene ethylene copolymers must also be affected by the incorporation of the ethylene unit in the crystalline lattice, but the exact dependence of $\Delta H_u$ with $X_c$ is unknown. However, if as suggested [73], a linear additive functionality is assumed ($\Delta H_{u\ copo} = \Delta H_u - \varepsilon X_c^{eq}$), the $\Delta H_u$ of the homopolymer will be only slightly decreased, by 0.1–0.7% in the range of ethylene content analyzed.

Table 3
Thermodynamic and structural parameters of α and γ iPP homopolymer crystals used in the analysis of the temperature coefficient of the linear growth rates

| α phase | γ phase |
|---|---|
| $T_m^\circ = 186.1$ °C [65] | $T_m^\circ = 187.2$ °C [65] |
| $\Delta H_u = 209$ J/g [65] | $\Delta H_u = 190$ J/g [65] |
| Crystal $\rho = 0.945$ g/cm$^3$ [66] | Crystal $\rho = 0.938$ g/cm$^3$ [21] |
| $a_0 = 5.49$ Å[a] [67] | $a_o = 6.46$ Å[b] [21,68] |
| $b_0 = 6.26$ Å[a] [67] | $b_0 = 5.29$ Å[b] [21,68] |
| $C_\infty = 5.7$ [54] | $C_\infty = 5.7$ |
| $l_b/l_u = 1.42$ [54] | $l_b/l_u = 1.42$ |

References for these values are given within brackets.
[a] Parameters for (1 1 0) growth plane.
[b] Parameters for growth along the *c* axis of the γ lattice.

[2] This value was obtained using the Clapeyron equation with estimated volume change with pressure [65].

[3] Specific NMR experiments pointed out that there is no preference in partitioning of the ethylene defect between α and γ crystallites. Therefore, the calculations of $T^\circ_{m\ copo}$ (α) and $T^\circ_{m\ copo}$ (γ) were carried out using the same set of $X_c$ data and $T^\circ_m$ and $\Delta H_u$ values specific of each polymorph [65], as listed in the text.

### 3.2. Analysis of the temperature coefficient of the linear growth rates

The spherulitic linear growth rates corresponding to the growth of α crystals are plotted according to Eq. (1) in Fig. 9. The data in this figure were calculated with $U^*=1500$ cal/mol $C_2=30$ K, $T_g=-15$ °C and values of $T^\circ_{m\ copo}$ and $\Delta H_u$ corresponding to the α phase. It is apparent that the data in the high $T_c$ and low $T_c$ regions display very similar gradients and can be represented by straight lines. There is not a clear demarcation of a break in the data that may correspond to two regimes with a ratio of slopes of 1/2 as predicted by the theory. The choice of the second set of 'universal' constants for the transport term ($U^*=4120$ cal/mol and $C_2=51.6$), changed the absolute value of the slopes for each copolymer but not the characteristic linearity of the gradient. The same unchanged behavior was observed if the $T^\circ_m$ of the homopolymer is taken as 200 °C or as high as 212 °C as suggested in earlier studies [55,63]. Only when the equilibrium melting temperature of the copolymers were arbitrarily lowered by 10–20° from the values listed in Table 2, was the analysis of $G$ according to Eq. (1) in accordance with a III to II regime transition. However, as described in the preceding section, such low $T^\circ_{m\ copo}$ values are not justified for the random propylene ethylene copolymers studied.

The same data shown in Fig. 9 are contrasted with the behavior of the homopolymer in Fig. 10. In agreement with other extensive data in ZN-based homopolymers [54,56] and fractions [40,55], the growth rates of metallocene iPP can be described according to a regime III to II transition. The ratio of the slopes in each regime is 1.9 and the transition between regimes takes place at $T_c=137$ °C, both values are in close agreement with theoretical predictions [54–56]. Added as open symbols are data corresponding to the linear growth rates obtained in the region of pure gamma growth for PE 1.8 and PE 2.8. These data were calculated with parameters corresponding to the gamma phase (Table 3). As seen in the figure, for PE 2.8 the data for pure γ growth falls on the same slope of the data at the low $T_c$ region, characteristic of the α growth. Although more scattered, the corresponding data for pure gamma growth in PE 1.8 appear to have a similar behavior. Hence, the growth mechanisms in both temperature regions must have the same nucleation rate dependence.

The correspondence of the copolymer crystallization behavior with any specific regime is not unambiguous, as apparent in this figure. By direct comparison with the homopolymer's temperature coefficient one could speculate that at the lowest $T_c$s the crystallization mechanism follows Regime III. However, it should be also considered that Regime I may be the only alternative mechanism for the γ phase since as stated, during γ growth it seems necessary to assume that an individual bilayer be completed before successive ones deposit on the growing surface [32]. Since the data for α and γ growth in Fig. 10 fall on the same line, it is plausible that the same mechanism govern the crystallization of both polymorphs.

The slopes of the straight lines drawn in Fig. 10 represent the temperature coefficient of growth of alpha lamellae (continuous lines) and gamma phase (dashed line) and can be used to calculate the product of the interfacial free energies ($\sigma\sigma_e$) corresponding to both types of crystallites, according to Eq. (2). To best represent pure structures, the data for α phase before the break are considered. A value of $Y=4$ corresponding to regimes I and III was used and the

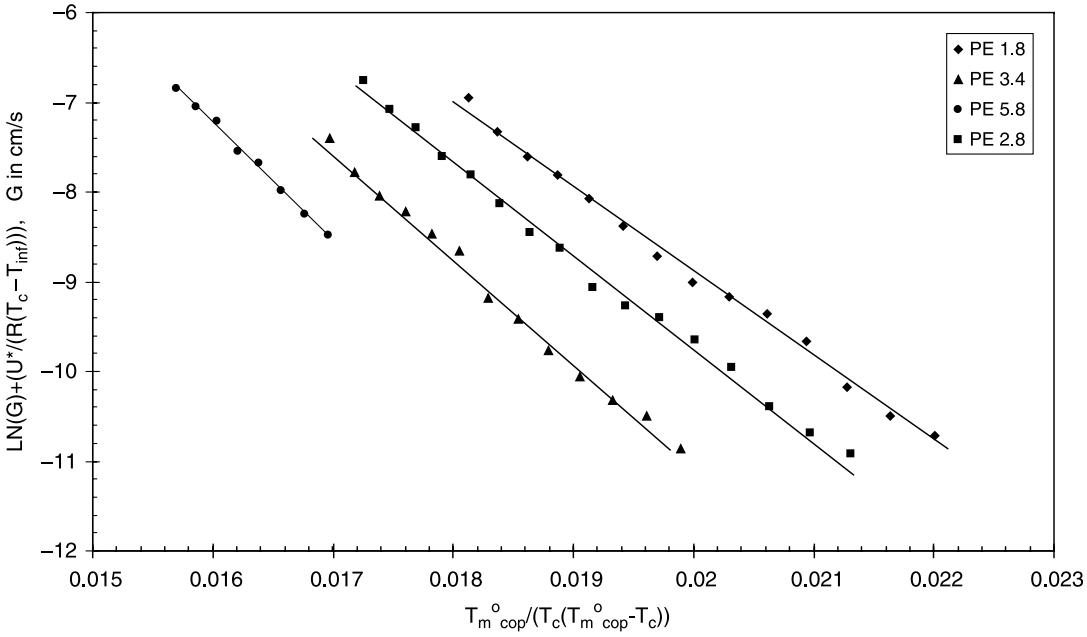


Fig. 9. Plot of the linear growth rates of α crystals according to Eq. (1) for the indicated propylene ethylene copolymers.

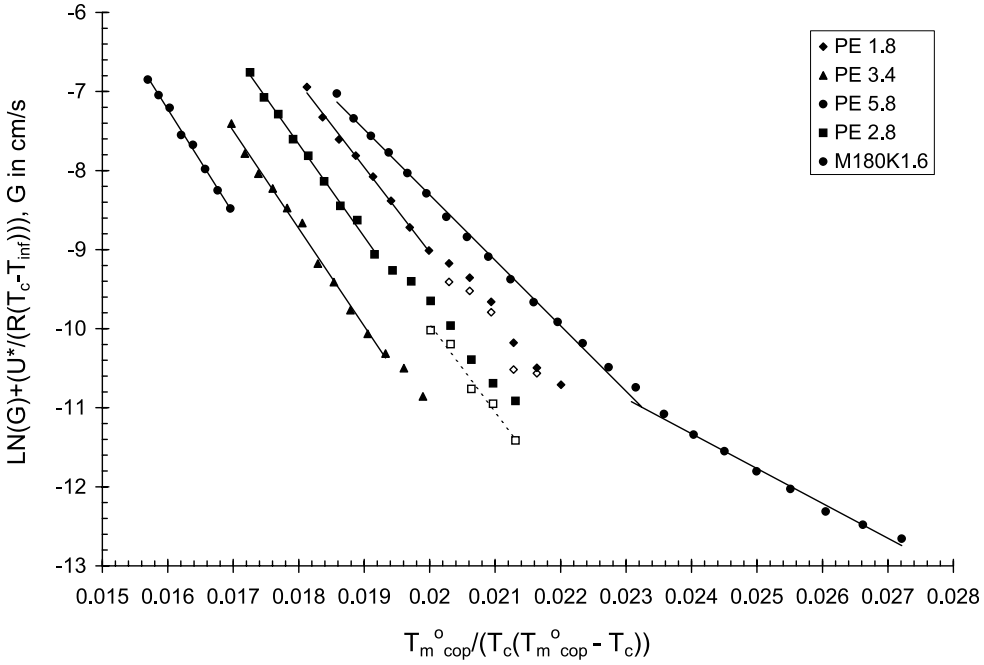


Fig. 10. Plot of the linear growth rates according to Eq. (1) for the indicated homopolymer and propylene ethylene copolymers. Filled symbols: α growth. Open symbols: γ growth.

parameters for α and γ crystals tabulated in Table 3. The lateral surface free energy, $\sigma$ was calculated according to the suggested relationship of this parameter and the characteristic ratio ($C_\infty$) of the poly(propylene) chain [74]

$$\sigma = \frac{a_0 \Delta H_u l_b}{2 l_u C_\infty} \quad (5)$$

in this expression $l_b$ is the C–C backbone length and $l_u$ the C–C distance as projected along the chain axis. Values of the slopes, the product ($\sigma\sigma_e$) and independent values of the lateral and surface free energies are listed for increasing ethylene content in Table 4. The calculated $\sigma$ and $\sigma_e$ values depend strongly on the choices of $T_m^\circ$ and $\Delta H_u$, hence, a comparison with literature values is only meaningful when the data are reanalyzed for the same thermodynamic parameters. We noticed that $\sigma_e$ obtained for the metallocene iPP studied here is identical to the value found by Clark and Hoffman in their analysis of $G$ data for various ZN iPPs

Table 4
Calculated interfacial free energies from lines of Fig. 10

| Ethylene (mol%) | Slope (K) | $\sigma\sigma_e$ (erg$^2$/cm$^4$) | $\sigma$ (erg/cm$^2$) | $\sigma_e$ (erg/cm$^2$) |
|---|---|---|---|---|
| 0 (Regime III) | 828 | 901 | 13.5 | 67 |
| 0 (Regime II) | 425 | 925 | 13.5 | 69 |
| 0.8 | 1075 | 1170 | 13.5 | 87 |
| 1.7 | 1172 | 1275 | 13.5 | 95 |
| 2.2 | 1235 | 1344 | 13.5 | 100 |
| 4.6 | 1315 | 1431 | 13.5 | 106 |
| 1.7 (γ) | 1132 | 1315 | 14.3 | 92 |

[54]. The product of interfacial free energies and, therefore, the value of the basal free energy ($\sigma_e$) increase substantially with increasing ethylene in the chain. Values of $\sigma_e$ range from 68 erg/cm$^2$ for the homopolymer to 106 erg/cm$^2$ for the 4.6 mol% copolymer, which correspond to a 56% increase with reference to the homopolymer. Since the majority of the ethylene units are excluded from the crystal, a natural conclusion, which parallels any partitioning model of these units in the intercrystalline region, is that they will tend to accumulate preferentially at the crystalline–amorphous interface. Hence, one possible interpretation is that the defects, accumulated preferentially at the basal (0 0 1) plane, lead to a more disordered and strained interface. This was the interpretation given in previous works [75]. Contrasting this view we question that the ethylene defect, of a smaller volume than the propene unit, could pose such a strain on the iPP crystal surface and propose that the increase of $\sigma\sigma_e$ with increasing ethylene may be related with the change in relative contents of α and γ phase with increasing $T_c$ among the copolymers. Although α growth is measured, simultaneous highly efficient gamma branching effectively changes $\sigma$ in unknown factors. Thus, one could speculate that it is perhaps $\sigma$ and not $\sigma_e$ that controls the change in $\sigma\sigma_e$ with increasing ethylene. In addition, growth in more than one lattice plane may occur if Regime III is operative in different proportions among the copolymers.

The interfacial free energies from the region of pure gamma growth for PE 2.8 are also listed in Table 4. The calculated value of $\sigma_{e(\gamma)} = 92$ erg/cm$^2$ is very similar to the alpha value of the same copolymer (95 erg/cm$^2$), and almost

double the $\sigma_{e(\gamma)}$ value obtained by Angelloz et al. [70] from the analysis of overall crystallization rates of iPP under high pressure. Mezghani and Phillips [65] listed $\sigma_{e(\alpha)}=52.2$ erg/cm$^2$ obtained with $\Delta H_{u(\alpha)}=209$ J/g and $\sigma_{e(\gamma)}=51.7$ erg/cm$^2$ obtained with $\Delta H_{u(\gamma)}=144.8$ J/g. However, these authors stated in the same work that for $\Delta H_{u(\alpha)}=209$ J/g the corresponding heat of fusion of the gamma phase should be 190 J/g. When the suggested $\Delta H_{u(\gamma)}=190$ J/g is used, the corrected $\sigma_{e(\gamma)}$ is 68 erg/cm$^2$, which is higher than the $\alpha$ value against all expectations [32].

Compared to the $\alpha$ crystal, the existence of non-parallel chain orientations in the $\gamma$ phase leads to $\sim$23% less number of chains leaving the crystal surface per unit area. Therefore, the increased surface area available per chain should project a decreased surface strain in the $\gamma$ crystals. The $\sigma_{e(\gamma)}$ obtained in our analysis does not reflect this expectation. Moreover, as anticipated in this work, this value is subject to further evidences for a direct correlation between the measured spherulitic $\gamma$ growth and the growth of $\gamma$ lamellae.

## 4. Conclusions

Analysis of the spherulitic linear growth rates of a series of metallocene based propylene ethylene copolymers, coupled with thermal and X-ray diffraction data of the simultaneous development of the $\alpha$ and $\gamma$ polymorphs, has allowed us to isolate the growth of pure $\gamma$ phase from that of mixed $\alpha$ and $\gamma$ crystals. The linear growth rate that corresponds to the pure $\gamma$ phase was found to be lower than that of the $\alpha$ supporting earlier suggestions based on the unusual packing of the $\gamma$ form.

The discontinuity observed in the temperature gradient of the growth of $\alpha$ crystals is associated with a change in crystallization mechanism at the changeover from an extended-like crystallization mechanism at high $T_c$s, where the fraction of crystals is dominated by the $\gamma$ phase, to a folded type mechanism at lower $T_c$s where both $\alpha$ and $\gamma$ prevail.

The analysis of the temperature coefficient of the kinetics of linear growth of the copolymers, according to nucleation theory, did not lead to a clear demarcation in the data that could be associated with different regimes in the crystallization mechanism. In the temperature domains where growth of pure $\alpha$ and $\gamma$ structures was isolated, the slopes of the temperature gradient are very similar, indicating the same nucleation rate dependence for the mechanism of growth of both forms. The values of the nuclei surface energies for $\alpha$ and $\gamma$ forms, extracted from the kinetic analysis, are very similar. Moreover, it is also discussed that the intimate structural relations between $\alpha$ and $\gamma$ polymorphs complicate the determination of these surface energies using growth kinetics. The $\alpha/\gamma$ relationships build up at the earliest stages of the crystallization.

## Acknowledgements

Funding of this work by the National Science Foundation, grant number DMR-0094485 and assistance of REU student Adrian Little with the polarized optical microscopy are gratefully acknowledged.

## References

[1] Monasse B, Haudin JM. Colloid Polym Sci 1988;266:679.
[2] Avella M, Martuscelli E, Della Volpe G, Segre A, Rossi E. Macromol Chem 1986;187:679.
[3] Laihonen S, Gedde UW, Werner P-E, Martinez-Salazar J. Polymer 1997;38:361.
[4] Feng Y, Hay JN. Polymer 1998;39:6589.
[5] Morini G, Albizzati E, Balbontin G, Mingozzi I, Sacchi MC, Forlini F, et al. Macromolecules 1996;29:5770.
[6] Xu J, Feng Y. Eur Polym J 2000;36:867.
[7] Alamo RG, Blanco JA, Agarwal P, Randall JC. Macromolecules 2003;36:1559.
[8] Scheirs J, Kaminsky W, editors. Metallocene-based polyolefins, vol. 2. Chichester: Wiley; 2000.
[9] Coates GW, Waymouth RM. Science 1995;267:217.
[10] Witte P, Lal TK, Waymouth RM. Organometallics 1999;18:4147.
[11] Wiyatno W, Chen ZR, Liu Y, Waymouth RM, Krukonis V, Brennan K. Macromolecules 2004;37:701.
[12] Brintzinger HH, Fischer D, Mulhaupt R, Rieger B, Waymouth RM. Angew Chem Int Ed Engl 1995;34:1143.
[13] Hosier IL, Alamo RG, Esteso P, Isasi JR, Mandelkern L. Macromolecules 2003;36:5623.
[14] Hosier IL, Alamo RG, Lin JS. Polymer 2004;45:3441.
[15] Alamo RG, VanderHart DL, Nyden MR, Mandelkern L. Macromolecules 2000;33:6105.
[16] Alamo RG, Kim M-H, Galante MJ, Isasi JR, Mandelkern L. Macromolecules 1999;32:4050.
[17] Brückner S, Meille SU, Petraccone U, Pirozzi B. Prog Polym Sci 1991;16:361.
[18] Lotz B, Wittman JC. J Polym Sci, Polym Phys Ed 1986;24:1541.
[19] Lotz B, Wittman JC, Lovinger AJ. Polymer 1996;37:4979.
[20] Lotz B. J Macromol Sci Part B 2002;B41:685.
[21] Meille SU, Brückner S, Porzio W. Macromolecules 1990;23:4114.
[22] Lotz B, Graff S, Straupe S, Wittman JC. Polymer 1991;32:2902. Lotz B, Graff S, Wittman JC. J Polym Sci B, Polym Phys 1986;24:2017. Lotz B, Wittman JC. Prog Colloid Polym Sci 1992;87:3.
[23] Turner-Jones A. Polymer 1971;12:487.
[24] Dai PS, Cebe P, Capel M. J Polym Sci, Polym Phys Ed 2002;40:1644.
[25] Lovinger AJ. J Polym Sci, Polym Phys Ed 1983;21:97.
[26] Tritto I, Fan Z-Q, Locatelli P, Sacchi MC, Camurati I, Galimberti M. Macromolecules 1995;28:3342.
[27] Randall RC. Macromolecules 1978;11:592.
[28] Busico V, Cipullo R, Monaco G, Vacatello M, Segre AL. Macromolecules 1997;30:6251.
[29] Kakugo M, Naito Y, Mizunama K, Miyakate T. Macromolecules 1982;15:1150.
[30] Turner-Jones A, Aizlewood JM, Beckett DR. Makromol Chem 1964;75:134.
[31] Alamo RG, Mandelkern L. Macromolecules 1991;24:6480.
[32] Meille SU, Ferro DR, Brückner S. Macrom Symp 1995;89:499.
[33] Morrow DR. J Macromol Sci Phys 1969;B3:53.
[34] Kovacs AJ, Gonthier A, Kolloid ZZ. Polymer 1972;250:530. Kovacs AJ, Gonthier A, Straupe C. J Polym Sci, Polym Symp 1975;50:283. Kovacs AJ, Straupe C, Gonthier A. J Polym Sci, Polym Symp 1977;59:31.
[35] Cheng SZD, Chen J, Janimak J. Polymer 1990;31:1018.

[36] Cheng SZD, Chen J. J Polym Sci, Polym Phys Ed 1991;29:311.
[37] Fatou JG, Marco C, Mandelkern L. Polymer 1990;31:890.
[38] Alamo RG, Mandelkern L, Stack GM, Kronke C, Wegner G. Macromolecules 1994;27:147.
[39] Ungar G. In: Lemstra PJ, Kleintjens IA, editors. Integration of fundamental polymer science and technology, vol. 2. London: Elsevier; 1988. p. 346.
[40] Janimak JJ, Cheng SZD, Giusti PA, Hsieh ET. Macromolecules 1991; 24:2253.
[41] Lauritzen Jr JI, Hoffman JD. J Appl Phys 1973;44:4340.
[42] Hoffman JD, Davis GT, Lauritzen Jr JI. In: Hannay NB, editor. Treatise on solid state chemistry. Treatise on solid state chemistry, vol. 3. New York: Plenum Press; 1976 [chapter 7].
[43] Hoffman JD. Polymer 1983;24:3.
[44] Hoffman JD, Miller RL. Polymer 1997;38:3151.
[45] Hillig WB. Acta Metall 1966;14:1868.
[46] Nielsen AE. Kinetics of precipitation. New York: Pergamon Press; 1964 p. 46.
[47] Calvert PD, Uhlmann DR. J Appl Phys 1972;43:944.
[48] Vogel H. Phys Z 1922;22:645.
[49] Fulcher GH. J Am Ceram Soc 1925;8:339.
[50] Tamman VG, Hesse HZ. Anorg Allg Chem 1926;19:245.
[51] Lovinger AJ, Davis GT, Padden Jr FJ. Polymer 1985;26:1595.
[52] Mandelkesn L. Crystallization of polymers, vol 2. Cambridge: Cambridge University Press, 2004. Boon J. Challa G. Van Krevelen DW. J Polym Sci Part A-2 1968;6:1835.
[53] Magill H. J Polym Sci Part A 1965;3. Magill H, Plazek. J Chem Phys 1965;3:1195.
[54] Clark EJ, Hoffman JD. Macromolecules 1984;17:878.
[55] Xu J, Srivatsan S, Marand H. Macromolecules 1998;31:8230.
[56] Monasse B, Haudin JM. Colloid Polym Sci 1985;263:822.
[57] Allen RC, Mandelkern L. Polym Bull 1997;17:473.
[58] Crist B. Polymer 2003;44:4563.
[59] Sanchez IC, Eby RK. Macromolecules 1975;8:638.
[60] Helfand E, Lauritzen Jr JI. Macromolecules 1973;6:631.
[61] Mandelkern L. Crystallization of polymers. vol. 1. Cambridge: Cambridge University Press; 2002.
[62] Yamada K, Hikosaka M, Toda A, Yamazaki S, Tagashira K. Macromolecules 2003;36:4790. Yamada K, Hikosaka M, Toda A, Yamazaki S, Tagashira K. Macromolecules 2003;36:4802.
[63] Fatou JG. Eur Polym J 1971;7:1057.
[64] Mezghani K, Campbell RA, Phillips PJ. Macromolecules 1994;27: 997.
[65] Mezghani K, Phillips PJ. Polymer 1998;39:3735.
[66] Krighbaum WR, Uematsu I. J Poly Sci Part A 1965;3:767.
[67] Natta G, Corradini P. Nuovo Cimento 1960;15(Suppl 1):9.
[68] Angelloz C, Fulchiron R, Douillard A, Chabert B, Fillit R, Vautrin A, et al. Macromolecules 2000;33:4138.
[69] VanderHart DL, Alamo RG, Nyden MR, Kim M-H, Mandelkern L. Macromolecules 2000;33:6078.
[70] Huang TW, Alamo RG, Mandelkern L. Macromolecules 1999;32: 6374.
[71] Alamo RG, Hosier IL. To be published.
[72] Fischer EW, Sterzel HJ, Wegner G, Kolloid ZZ. Polymer 1973;251: 980.
[73] Cheng SZD, Janimak JJ, Zhang A, Hsieh ET. Polymer 1991;32:648.
[74] Hoffman JD. Polymer 1992;33:2643.
[75] Galante MJ, Mandelkern L, Alamo RG, Lehtinen A, Paukkeri R. J Thermal Anal 1996;47:913.